

Effects of vertical control on anatomic and aerodynamic characteristics of the oropharyngeal airway during premolar extraction treatment of Class II hyperdivergent nonsevere crowding malocclusion

Hongyi Tang, Xinyu Cui, Huazhi Li, Fu Zheng, Youchao Chen, and Jiuhi Jiang
Beijing, China

Introduction: This study aimed to analyze the effects of premolar extraction treatment with vertical control on changes in the anatomy and aerodynamics of the oropharynx in Class II hyperdivergent malocclusion with non-severe crowding. **Methods:** Thirty-nine patients with Class II hyperdivergent malocclusion were enrolled consecutively. All the participants underwent 4 premolar extractions. The high-pull J-hook and mini-implants were used to provide vertical control. Cone-beam computed tomography was performed before and after treatment. The participants were divided into a decreased lower vertical facial height group ($n = 23$) and an increased lower vertical facial height group ($n = 16$) on the basis of superimposition. The aerodynamic characteristics, including airway resistance (inspiration, R_{in} ; expiration, R_{ex}) and maximum velocity (inspiration, $V_{max_{in}}$; expiration, $V_{max_{ex}}$) at inspiration and expiration, were calculated using computational fluid dynamics. Anatomic characteristics, including volume and cross-sectional area (CSA_{min}), were measured using the Dolphin Imaging software (Dolphin Imaging and Management Solutions, Chatsworth, Calif). **Results:** After treatment, the median volume and CSA_{min} increased by 2357 mm^3 and 43 mm^2 , respectively, and median R_{in} and $V_{max_{ex}}$ decreased by 0.15 Pa/L/min and $0.24 \text{ m} \times \text{s}^{-1}$, respectively, in decreased lower vertical facial height group. In contrast, the median CSA_{min} decreased by 9.5 mm^2 in the increased lower vertical facial height group. All the changes were statistically significant (all $P < 0.05$). Significant differences in volume, CSA_{min} , R_{in} , and $V_{max_{ex}}$ were observed between the 2 groups. **Conclusions:** Vertical control might improve the anatomic and aerodynamic characteristics of the oropharyngeal airway during premolar extraction treatment of Class II hyperdivergent malocclusion with nonsevere crowding. (Am J Orthod Dentofacial Orthop 2023;164:e27-e42)

Obststructive sleep apnea (OSA) is a respiratory physiological disorder characterized by recurrent apnea and hypopnea that can lead to snoring,

hypoxia, and arousal from sleep.¹ OSA can also increase the risk of hypertension, diabetes, cardiovascular, and respiratory diseases.^{2,3} The pathogenesis of OSA remains unclear⁴; however, the anatomic and functional abnormalities of the upper airway may be important factors contributing to OSA.^{5,6} It has been reported that Class II hyperdivergent malocclusion may be associated with anatomic and functional defects of the upper airway because of mandibular deficiency and a steep mandibular plane, and thus, it can increase the risk of OSA.⁷⁻⁹ Therefore, the upper airway of such patients should be monitored carefully during treatment.

Premolar extraction is a conventional camouflaged orthodontic method for treating Class II hyperdivergent

From the Department of Orthodontics, Peking University School and Hospital of Stomatology, Beijing, China.

All authors have completed and submitted the ICMJE Form for Disclosure of Potential Conflicts of Interest, and none were reported.

The study was approved by the ethics committee of the School of Stomatology, Peking University (no. 2021-09-68-26).

Address correspondence to: Jiuhi Jiang, Department of Orthodontics, Peking University School and Hospital of Stomatology, #22 Zhongguancun S Ave, Haidian District, Beijing, China 100081; e-mail, drjiangw@163.com.

Submitted, March 2022; revised and accepted, May 2023.

0889-5406/\$36.00

© 2023.

<https://doi.org/10.1016/j.ajodo.2023.05.003>

malocclusion, which is used to align dentition, improve protrusion of anterior teeth, and adjust the intermaxillary relationship.¹⁰ There is no consensus on the effects of premolar extraction on the upper airway. Some studies reported that extraction orthodontic treatment decreased the upper airway size because of the reduction in arch length and oral cavity size.^{11,12} But Zhang et al¹³ found that the upper airway was only adjusted adaptively rather than a decrease in size. A related study found that extraction orthodontic treatment combined with vertical control increased the size of the oropharyngeal airway because the treatment caused significant upward movement of the mandible.¹⁴ Therefore, analyzing the changes in the upper airway characteristics after premolar extraction treatment is necessary.

Vertical control is important in treating Class II hyperdivergent malocclusion because it promotes counterclockwise rotation of the mandible and decreases lower vertical facial height (LVFH).^{14,15} In addition, several studies have indicated that vertical control benefits the upper airway in different treatments, including orthognathic surgery and rapid maxillary expansion.^{16,17} Therefore, it is valuable to investigate the effects of vertical control on the upper airway after premolar extraction treatment to correct Class II hyperdivergent malocclusion.

Computational fluid dynamics (CFD) has been widely used to simulate the airflow of the upper airway on the basis of a 3-dimensional (3D) reconstructed model from cone-beam computed tomography (CBCT).^{16,18,19} It can provide quantitative parameters by showing the contours of aerodynamic characteristics such as pressure drop and velocity, which can be used to evaluate the respiratory function of patients.^{16,20}

To our knowledge, only 1 study has reported on the changes in the upper airway after premolar extraction treatment with a vertical control. In that study, comparisons were made before and after treatment, but no comparisons were made between different groups.¹⁴ Furthermore, previous studies have not used CFD to evaluate the changes in aerodynamic characteristics of the upper airway after premolar extraction treatment. Therefore, we performed intergroup comparisons to test the hypothesis that effective vertical control benefits the anatomy and aerodynamics of the upper airway after premolar extraction treatment.

MATERIAL AND METHODS

Based on data on airway changes in a previous study,²¹ a power calculation determined that 16 subjects were needed in each group to achieve a power of 80%. Between April 2016 and February 2022, 49 patients

with Class II hyperdivergent malocclusion who had undergone premolar extraction treatment at Peking University School of Stomatology were enrolled in this retrospective study. The inclusion criteria were (1) aged >18 years, (2) the patients were diagnosed with hyperdivergent Class II malocclusion ($ANB >4^\circ$, $MP/SN >37^\circ$), (3) orthodontic treatment with extraction of the 4 premolars was assisted by a J-hook with mini-implants, and (4) normalized orthodontic results were achieved including Class I canine and molar relationships, a normal overbite, and a normal overjet. The exclusion criteria were (1) visible figure differences before and after treatment (because obesity may be a confounding factor, we collected facial front photographs of all the subjects, which 2 researchers assessed); we asked the researchers (F.Z. and Y.C.C.) if they could see a difference between the before and after treatment photographs of each subject. If researchers could not detect a difference, the difference was considered small/negligible); (2) severe dentofacial anomalies, such as cleft lip or palate; (3) Temporomandibular joint discomfort and limited mouth opening (the medical records were reviewed to ensure that there were no documented symptoms before and after treatment); (4) congenital loss of permanent teeth; (5) previous orthodontic treatment and/or orthognathic surgery; and (6) severe crowding (>8 mm crowding level of each arch). In the case of severe overcrowding, the extraction space is mainly used to solve the overcrowding problem. Conversely, in the case of nonsevere overcrowding, the extraction space is mainly used to guide the direction of tooth movements (sagittal and vertical). Patients with severe crowding have different needs regarding dental movement directions and distances than those with less severe crowding.

Two patients were excluded because of severe crowding, 2 because of visible figure difference, 1 because of congenital loss of permanent teeth, and 5 because of a lack of relevant CBCT data. Finally, 39 patients (aged 26.65 ± 7.69 years; 15 men and 24 women) were included. Before this retrospective study, the CBCTs of all patients had been taken to evaluate their malocclusion problems and provide more appropriate treatment and were electronically archived at the hospital, so we did not collect informed consent from the patients. We explained this to the Ethics Committee of Peking University School of Stomatology and obtained permission (No. 2021-09-68-26).

After premolar extractions, all patients were actively treated using 0.022-inch edgewise brackets (Shinye Medical Technology, Zhejiang, China). High-pull J-hook (Shinye Medical Technology, Zhejiang, China) was applied to the anterior part of the dental arch to

provide sagittal and vertical control of the dental anterior arch. We applied both maxillary and mandibular J-hooks. The J-hooks were used alternately. The specific standards were as follows. The maxillary J-hook was used to close only the maxillary extraction space, simultaneously close the maxillary and mandibular extraction space, and adjust precisely after closing the extraction space. The mandibular J-hook was used to close only the mandibular extraction space. Closing extraction spaces in the maxilla and mandible may not completely overlap in time; therefore, a mandibular J-hook was used when only the mandibular extraction spaces were closed. Two mini-implants were inserted bilaterally in the zygomatic alveolar ridge between the maxillary first and second molars to assist the maxillary dentition intrusion. These 2 methods were used to provide vertical control during the treatment. The elastic traction forces applied by the J-hook and mini-implants were 400-500 g and 100-150 g of force, respectively. After aligning the dentition, we continued the treatment with stainless steel wires to facilitate traction. The duration of anterior teeth retracted with traction forces was approximately 10-14 months, and the duration of the maxillary molars intruded with traction forces was approximately 6-8 months. The treatment duration varied from 30-36 months. After treatment completion, we evaluated the effects of the vertical control on the basis of cranial base superimpositions observed in imaging. This is a standard method for evaluating skeletal changes after orthodontic treatment.²² For the analyses, we divided the participants into 2 groups: (1) the decreased LVFH (D-LVFH) group (9 men and 14 women) and (2) the increased LVFH (I-LVFH) group (6 men and 10 women).

CBCT scans (DCT PRO Dentofacial CBCT System; Vatech Co, Seoul, South Korea) were taken before and after treatment for each participant (CBCT device was set at 90 kV, 7 mA, a field of view of 20 cm × 19 cm, voxel size of 0.40 mm, and scan time of 15 seconds). Each participant was scanned upright, keeping the Frankfort horizontal plane (FHP) parallel to the floor, the teeth in centric occlusion, and the tongue in the position at the end of swallowing (ie, against the palate). The participants were also instructed to breathe smoothly and not swallow.¹⁵ An instructor guided the CBCT imaging process by instructing the patient to remain upright. All CBCT data were saved in digital imaging and communications in medicine file format.

All measurements were performed using Dolphin Imaging software (version 19.5; Dolphin Imaging and Management Solutions, Chatsworth, Calif). The digital imaging and communications in medicine file format

from the CBCT images were imported into Dolphin Imaging software. The images were reoriented along the midpalatal suture tangent to the nasal base and parallel to the FHP. Lateral cephalograms were derived from the CBCT images to evaluate the dental and skeletal parameters. Figure 1 shows the dental and skeletal parameters. Three-dimensional cranial base superimposition was performed according to a previous study.²² The 3D cranial base superimposition diagram is shown in Figures 2 and 3. We also performed cephalometric superimpositions to further evaluate the dental and skeletal changes in both groups. The diagram of the cephalometric superimpositions is shown in Figure 4.

We selected the oropharyngeal airway as the object for evaluation and analysis. The following process was used to automatically reconstruct the volume using the Dolphin Imaging software: the airway range was measured by tracing the points and connecting them with lines to form a closed graph through the median sagittal plane, coronal plane, and cross-section. Then, we clicked the “seed point” button to place the yellow dots within the closed airway range. Then, we uniformly adjusted the gray value to 55 and automatically filled the calculated volume. After filling the selected area, we clicked the “update volume” button to obtain the volume of the upper airway. The related definitions and descriptions are presented in Table 1 and Figures 5 and 6.

The CBCT data were imported into Mimics Research software (version 19; Materialise, Leuven, Belgium). The gray value of the computed tomography (CT) images reflects the different attenuation coefficients of tissues to x-rays.²³ In general, tissues with a high density have a large attenuation to x-rays, and thus, the gray value of the CT images is large. The gray value of the CT images indicates the absolute value of the x-ray attenuation of the substance. Historically, Hounsfield set the CT value of water at 0 for convenience.²⁴ The CT value was converted according to this scale and is called Hounsfield units (HU). In human tissues, fat is approximately -100 HU, cancellous bone is approximately 100-300 HU, and compact bone is approximately 2000 HU. As air density is lower than other human tissues, the HU corresponding to the upper airway is lower than those of other tissues in the body. Many studies have used HU in CBCT evaluations for generating 3D models of the upper airway.^{25,26} After evaluating the appropriate HU threshold, we set our HU threshold between -1024 HU and -480 HU to highlight the oropharyngeal airway. All 3D models were exported as stereolithography files (Fig 7).

Many procedures of this section are derived from the study of Tang et al.¹⁶ All models were imported into

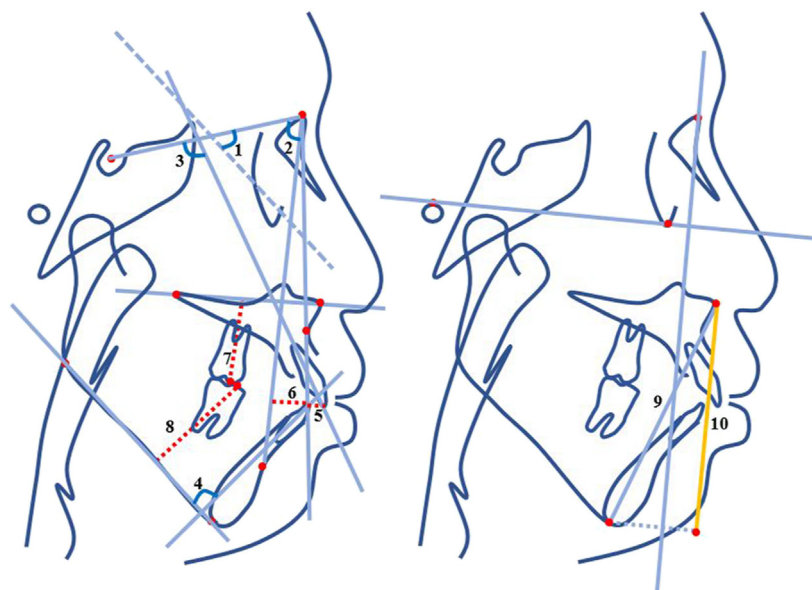


Fig 1. Skeletal and dental parameters: 1, MP/SN; 2, SNB; 3, U1/SN; 4, L1/MP; 5, U1-NA; 6, L1-NB; 7, U6-PP; 8, L6-MP; 9, ANS-Me; 10, LVFH.

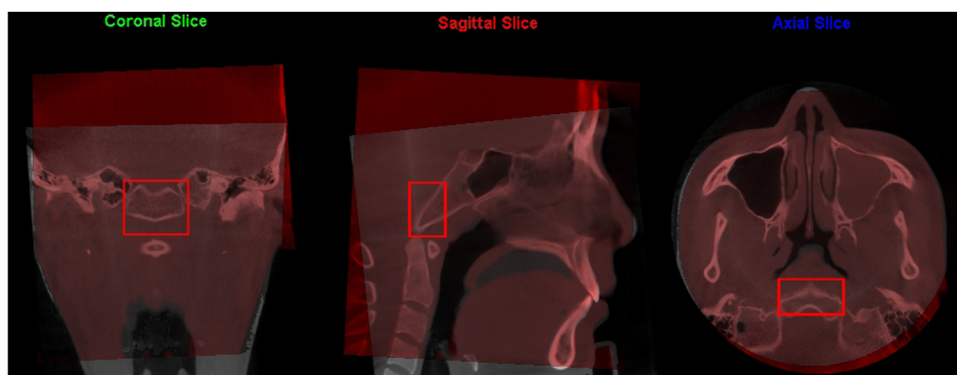


Fig 2. The cranial base part used for superimposition.

ICEM (version 19.1; ANSYS, Canonsburg, Pa) to generate a tetrahedral volume mesh. A typical grid consisted of approximately 2,500,000 tetrahedral cells, depending on the complexity of the oropharyngeal airway model (Fig 8).¹⁶

After mesh generation, the 3D mesh was exported into FLUENT (version 19.1; ANSYS, Canonsburg, Pa) for the airflow simulation. We applied the steady-state Reynolds-averaged Navier–Stokes formulation combined with the laminar model to analyze the aerodynamic characteristics of the oropharyngeal airway.^{16,27} The SIMPLE algorithm was used to realize the coupling between velocity and pressure, and second-order

discretization schemes were adopted.^{16,28} The air density and viscosity were set to 1.225 kg/m^3 and $1.79 \times 10^{-5} \text{ kg/m/s}$, respectively, which are the default settings of the system. An inlet volume flow rate of $166 \text{ mL} \times \text{s}^{-1}$ ($10 \text{ L} \times \text{min}^{-1}$) was set for the airflow simulation in an awake state.^{16,28} The air within the upper airway was assumed to be adiabatic.^{16,29} In the inspiration phase, the inlet boundary was set at the plane across the posterior nasal spine parallel to the FHP, and the outlet boundary was set at the plane across the tip of the epiglottis parallel to the FHP.¹⁶ In contrast, the expiration phase was simulated by setting the inlet at the plane across the tip of the epiglottis parallel to the FHP and the outlet at the plane

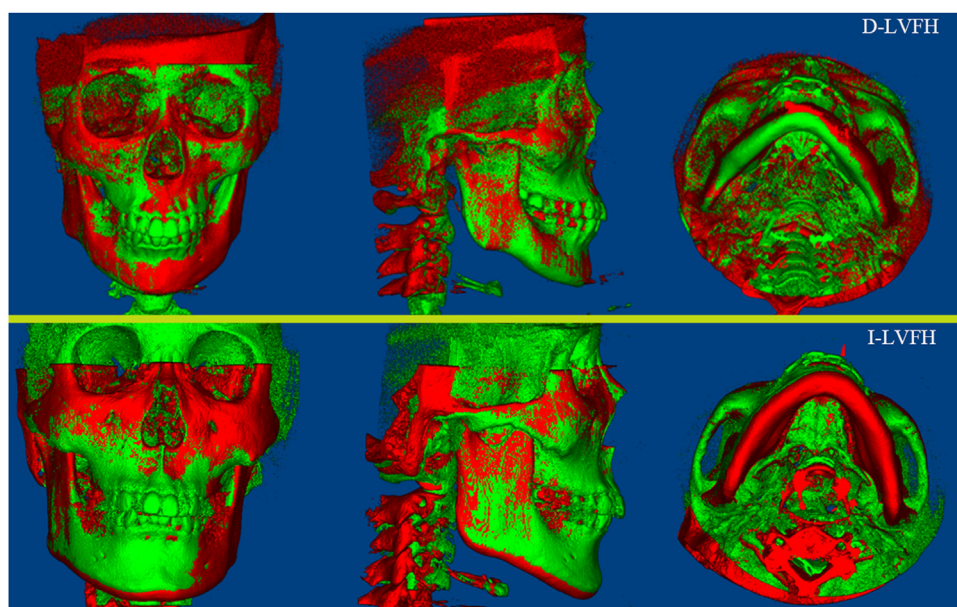


Fig 3. Diagram of superimposition (*green*, pretreatment; *red*, posttreatment): D-LVFH group; I-LVFH group.

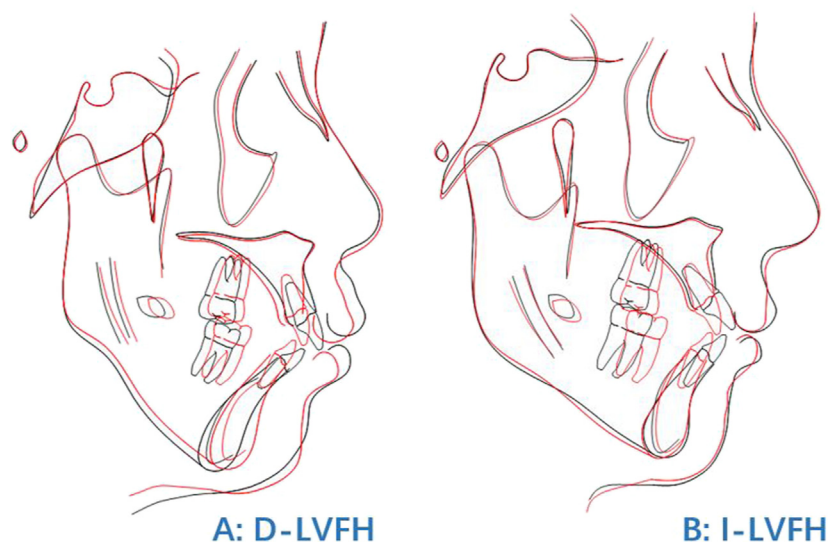


Fig 4. Diagram of cephalometric superimposition (*black*, pretreatment; *red*, posttreatment).

across the posterior nasal spine parallel to the FHP. The number of iterations is set to 400.¹⁶

The airway resistance (R) was computed on the basis of CFD calculations using the following formula: $R = \Delta P/Q$. ΔP (total pressure drop between the inlet and outlet boundaries of the oropharyngeal airway) = $P_{\max} - P_{\min}$.¹⁶ Q is the oropharyngeal inlet volume flow rate, which is constant.¹⁶

Statistical analysis

In this study, all parameters were remeasured by the same investigator after 2 weeks to determine if there was any internal operator error. Specifically, all cephalometric landmarks were relocated again, and all the oropharyngeal airway volumes were measured again to obtain a second set of results. As the measurements of CSA_{\min} and all aerodynamic parameters were stable

Table I. Descriptions and definitions

<i>Variables</i>	<i>Definitions</i>
Anatomic parameters	
S	Sella, the midpoint of the cavity of sella turcica
N	Nasion, the anterior point of the intersection between the nasal and frontal bones
Go	Gonion, the midpoint connecting the ramus and body of the mandible
Me	Menton, the most interior point on the chin
A	The deepest point on the concavity of the maxilla between ANS and the maxillary alveolus
B	The innermost point on the contour of the mandible between the mandibular incisor and chin
ANS	Anterior nasal spine
PNS	Posterior nasal spine
U6 occlusal point	Mesial buccal cusp tip of the maxillary first molar
L6 occlusal point	Mesial buccal cusp tip of the mandibular first molar
PP	The palatal plane, the plane connecting point ANS and point PNS
MP	The mandibular plane, the plane connecting point Go and point Me
SN	The line from point S to point N
MP/SN	The angle between the MP plane and the SN plane
SNB	The angle between point S, point N, and point B
U1/SN	The angle between the long axis of U1 and SN plane
L1/MP	The angle between the long axis of L1 and MP plane
U1-NA	The perpendicular distance from the U1 to N-A line
L1-NB	The perpendicular distance from the L1 to N-B line
U6-PP	The perpendicular distance from the U6 occlusal point to the ANS-PNS plane
L6-MP	The perpendicular distance from the L6 occlusal point to the mandibular plane
ANS-Me	The distance between point ANS and point Me
LVFH	ANS-Me (perp Frankfurt horizontal plane) Perpendicular distance between point ANS and point Me to Frankfurt horizontal plane
CSA _{min}	The minimum cross-sectional area of the upper airway
Total volume	Upper airway section between the line across PNS (posterior nasal spine) parallel to FHP and the line passing across the tip of epiglottis parallel to FHP
3D model of upper airway	
Superior boundary	The line across PNS parallel to FHP
Inferior boundary	The line passing across the tip of the epiglottis parallel to FHP
Pa/L/min	In the process of simulating the airflow in the upper airway, the pressure difference between the inlet and outlet of each liter of airflow through the upper airway in every minute
$m \times s^{-1}$	The assessment of meters of airflow per second during the process of simulating the airflow in the upper airway
ΔP	Total pressure drops between the inlet and outlet boundary of the oropharynx
Q	Inlet volume flow rate, which is set to $10 L \times \text{min}^{-1}$ (Constant)
R	$R = \Delta P/Q$
V_{max}	Maximum airflow velocity of the upper airway during airflow simulation
Interquartile range (IQR)	All values are arranged from small to large and divided into quartiles. The values at the 3 dividing points are quartiles. The interquartile range is the difference between the third quartile and the first quartile

and reproducible, the measurements were considered error-free. After summarizing the data, the intraclass correlation coefficient was calculated and was between 0.94-0.98; thus, data reliability was confirmed.

After inspection, all the data were analyzed using SPSS (version 23.0; IBM, Armonk, NY). Because the total number of selected patients was <40, we used Fisher's exact probability to compare the sex difference between the 2 groups. The normality of the data was tested using the Kolmogorov-Smirnov test. The average and standard deviation were used to describe data conformed to a normal distribution. The median and interquartile range were applied for data that did not conform to a normal distribution. The paired *t* test and independent sample *t*

test were used to compare normally distributed data, whereas the Wilcoxon signed rank test and Wilcoxon rank-sum test were used for analyzing data that were not normally distributed. The statistical significance level was set at $P < 0.05$.

RESULTS

The Kolmogorov-Smirnov test showed that SNB, ANS-Me, LVFH, U1-SN, U1-NA, L1-NB, L1-MP, U6-PP and L6-MP conformed to a normal distribution (Supplementary Table I). Thus, we used a parametric test to evaluate these measurements, whereas the others were assessed using nonparametric tests.

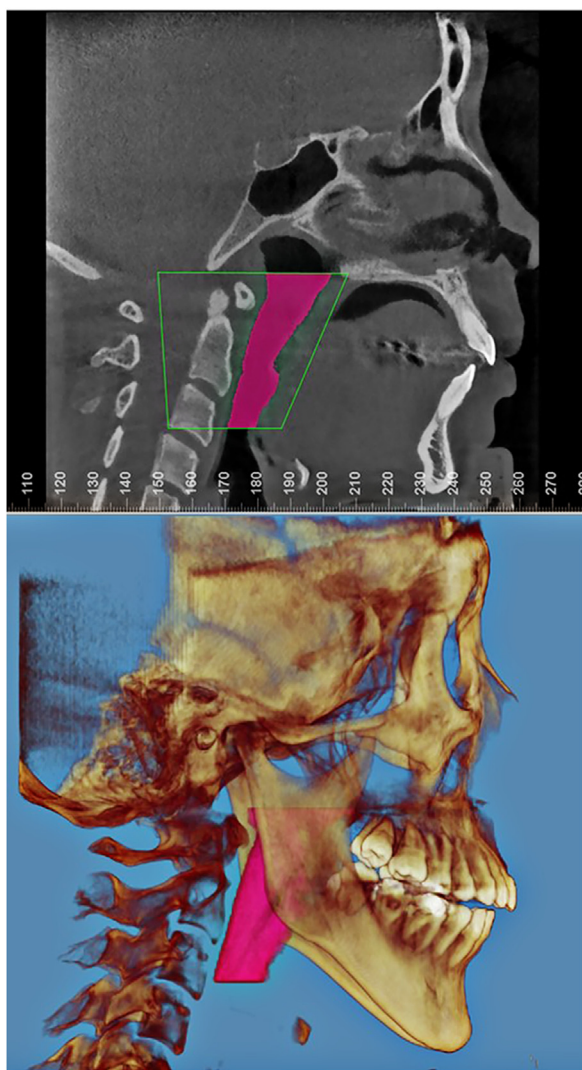


Fig 5. Volume of oropharyngeal airway (purplish-red).

We compared all parameters between the 2 groups at the pretreatment stage, and no significant differences were found (Table II). The comparisons before treatment also showed no significant differences in sex, body mass index, or crowding between the 2 groups (Table III).

Figure 9 shows opposite morphologic changes in the oropharyngeal airway between the D-LVFH and I-LVFH groups. Figures 10 to 13 show the pressure drop contours and maximum velocity streamlines during the inspiratory and expiratory phases in both groups.

In the D-LVFH group, the MP/SN decreased by 2.10° , LVFH decreased by 1.51 mm, and SNB increased by 1.23° (Table IV; $P < 0.05$). Significant increases in the volume and CSA_{\min} were observed (Table V; $P < 0.05$). The volume increased by $2,357 \text{ mm}^3$, and CSA_{\min}

increased by 43 mm^2 . R_{in} and $V_{\text{max}_{\text{ex}}}$ were reduced by 0.15 Pa/L/min and $0.24 \text{ m} \times \text{s}^{-1}$, respectively.

In the I-DVFH group, MP/SN and LVFH increased by 0.30° and 1.01 mm, respectively, and no significant change was found for SNB (Table IV; MP/SN and LVFH: $P < 0.05$; SNB: $P = 0.921$). CSA_{\min} decreased by 9.5 mm^2 (Table V; $P < 0.05$). The other oropharyngeal parameters showed decreasing trends in anatomy and an increasing trend in aerodynamics (Tables V and VI; variation, inspiration: R_{in} , 0.06 Pa/L/min ; $V_{\text{max}_{\text{in}}}$, $0.05 \text{ m} \times \text{s}^{-1}$; expiration: R_{ex} , 0.01 Pa/L/min ; $V_{\text{max}_{\text{ex}}}$, $0.30 \text{ m} \times \text{s}^{-1}$; volume, 343 mm^3 ; $P = 0.063\text{--}0.460$).

A significant maxillary molar intrusion was observed in the D-LVFH group, and significant maxillary molar extrusion was found in the I-LVFH group (Table IV; D-LVFH group: U6-PP, -1.40 mm ; $P < 0.05$; I-LVFH group: U6-PP, 0.77 mm ; $P < 0.05$). No significant vertical changes of mandibular molar were found in both groups (Table IV; D-LVFH group: L6-MP, -0.13 mm ; $P = 0.565$; I-LVFH group: L6-MP, 0.36 mm ; $P = 0.107$). In addition, similar anterior tooth retraction was observed in the 2 groups after treatment completion (Table 4; D-LVFH group: U1/SN, -4.05° ; L1/MP, -3.24° ; I-LVFH group: U1/SN, -5.29° ; L1/MP, -3.58° ; $P < 0.05$). Significant differences related to maxillary molars' vertical movements were observed between the 2 groups (Table VI; $P < 0.05$), but no significant differences related to other tooth movements were found (Table VI; $P = 0.118\text{--}0.881$).

We observed significant differences in the aerodynamic and anatomic characteristics, as represented by R_{in} , $V_{\text{max}_{\text{ex}}}$, CSA_{\min} , and volume of the oropharyngeal airway, between the 2 groups ($P < 0.05$). The D-LVFH group showed a significant decrease in aerodynamics and improved anatomic characteristics. Moreover, the I-LVFH group showed an opposite trend compared with the I-LVFH group (Table VI).

DISCUSSION

In this study, we compared the aerodynamic and anatomic changes of the oropharyngeal airway after pre-molar extraction for orthodontic treatment, with or without vertical control. The results suggest that pre-molar extraction with effective vertical control can improve the aerodynamic and anatomic characteristics of the oropharyngeal airway. Although we tried our best to provide orthodontic treatment to each patient, the effect of vertical control varied between the 2 groups. We speculated that treatment compliance may be an important consideration. Although we provided specific guidance to our patients for applying the J-hook, some patients failed to follow the instructions correctly. Moreover,

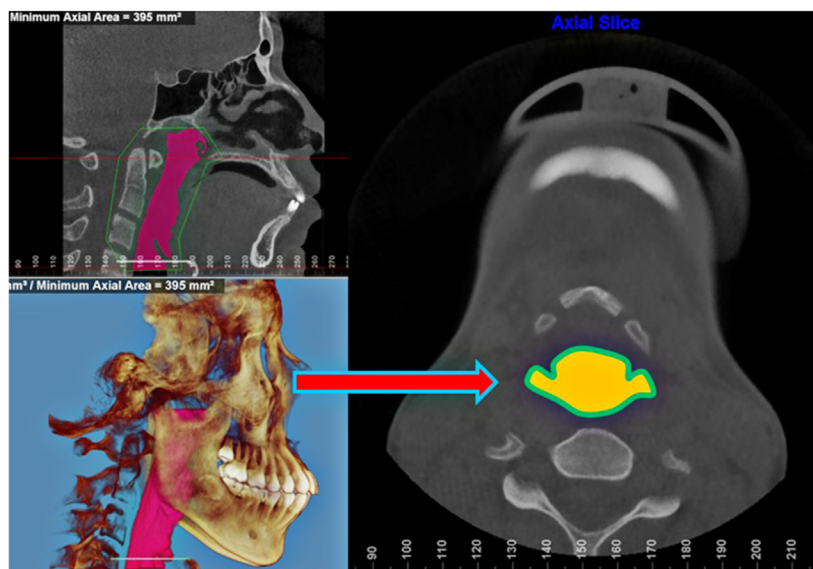


Fig 6. Minimum cross-sectional area (yellow).

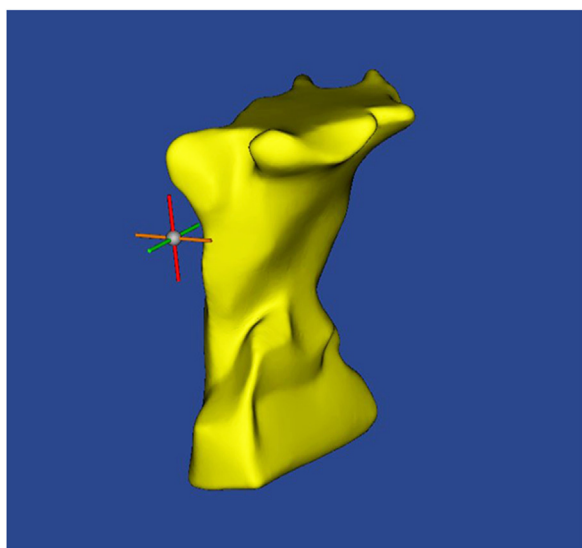


Fig 7. Three-dimensional reconstructed model of oropharyngeal airway.

some patients forgot to attend their orthodontic treatment appointments, which extended the treatment intervals. If the treatment intervals were prolonged, the elastic traction on the mini-implant may break and lose its function.

The interval between CBCT shooting is at least 30 months; hence, the harm of radiation exposure is negligible. A related study illustrated that between 8 and 18 years old, the volume of the human upper airway

increased with age.³⁰ Considering this, we selected adults as subjects.

The pretreatment comparisons of sex, body mass index (BMI), crowding level, and all measurable parameters did not differ significantly between the 2 groups (Tables II and III), indicating that the 2 groups were comparable.

The change of U6-PP showed that the vertical direction of maxillary molars in the 2 groups was opposite, indicating that the vertical direction of maxillary molars might be the determining factor of LVFH change. Previous studies have reported that molar intrusion is an important step to achieve vertical control,^{14,31} and our findings confirm the results. Unlike the maxillary molars, mandibular molars showed no significant vertical movement, possibly because of only maxillary mini-implants in the treatment process. It is recommended to consider using bimaxillary mini-implants in orthodontic treatments that require vertical control.

The changes in dental parameters, including U1/SN, L1/MP, U1-NA, and L1-NB, indicated significant retraction of the anterior teeth in both groups. Although the changes in the upper airway were different in the previous premolar extraction treatment studies, the results of dental parameters are roughly the same.^{10,13,14} Because of a similar amount of retraction of the anterior teeth in both groups, tooth movements were also not significantly different between the 2 groups. This similarity indicated there was no need to consider the changes in tooth movement as a confounder.

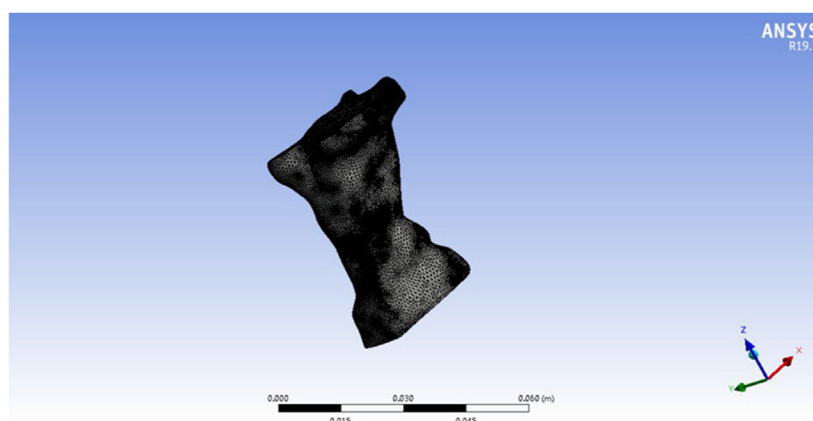


Fig 8. Generated tetrahedral volume mesh of oropharyngeal airway.

Table II. Comparison of pretreatment measurable parameters between the D-LVFH and I-LVFH groups

Parameters	D-LVFH group	I-LVFH group	P value
Skeletal and dental parameters			
SNB (°)	75.43 ± 2.77	75.96 ± 2.27	0.516
U1/SN (°)	102.67 ± 6.32	106.56 ± 8.72	0.139
U1-NA (mm)	5.02 ± 2.45	6.44 ± 2.20	0.068
L1/MP (°)	96.36 ± 5.60	97.01 ± 7.75	0.776
L1-NB (mm)	8.27 ± 2.85	8.87 ± 2.28	0.467
U6-PP (mm)	23.86 ± 2.61	23.61 ± 2.84	0.774
L6-MP (mm)	32.26 ± 2.96	31.20 ± 3.25	0.307
ANS-Me (mm)	70.83 ± 5.32	68.18 ± 4.91	0.119
LVFH (mm)	65.60 ± 4.74	64.06 ± 4.90	0.732
MP/SN (°)	39.70 (9.80)	38.65 (6.70)	0.525
Upper airway-anatomic parameters			
Oropharyngeal volume (mm ³)	16,612.00 (4692.00)	18,985.00 (13,219.75)	0.601
CSA _{min} (mm ²)	177.00 (147.00)	179.00 (136.75)	0.101
Aerodynamic parameters			
Airway resistance during inspiration (Pa/L/min)	0.64 (0.79)	0.46 (1.21)	0.601
Maximum velocity during inspiration (m × s ⁻¹)	2.19 (1.29)	1.60 (1.32)	0.079
Airway resistance during expiration (Pa/L/min)	0.60 (1.10)	0.53 (0.76)	0.966
Maximum velocity during expiration (m × s ⁻¹)	1.81 (2.03)	1.36 (1.62)	0.288

Note. Values are presented as mean ± standard deviation for normal distributions and median (interquartile range) for nonnormal distributions. Independent sample *t* test was used for normal distributions and Wilcoxon rank-sum test was used for nonnormal distributions.

Table III. Gender, BMI, and crowding level evaluation between the D-LVFH and I-LVFH groups

Characteristics	D-LVFH group	I-LVFH group	P value
Gender			
Male	9 (39.1)	6 (37.5)	>0.999
Female	14 (60.9)	10 (62.5)	
BMI (kg/m ²)	19.97 ± 2.18	21.03 ± 2.37	0.168
Crowding levels (mm)			
Maxillary	2.70 ± 1.55	2.94 ± 1.56	0.637
Mandibular	3.17 ± 1.72	3.19 ± 1.87	0.982

Note. Values are n (%), or mean ± standard deviation. Fisher exact test was used for gender, and independent sample *t* test was used for BMI and crowding levels.

Cranial base superimposition is a standard method for evaluating the rotational changes of the mandible after orthodontic treatment.²² Therefore, on the basis of this method, we divided the patients into 2 groups. We also used MP/SN and LVFH as the basic parameters for describing the effects of vertical control. In the D-LVFH group, both MP/SN and LVFH showed a favorable decrease. A decrease in MP/SN and LVFH represented the counterclockwise rotation of the mandible and a decrease in vertical facial height in the D-LVFH group. The application of superimposition and the reduction in MP/SN and LVFH ensured the measurement reliability of “effective vertical control.”

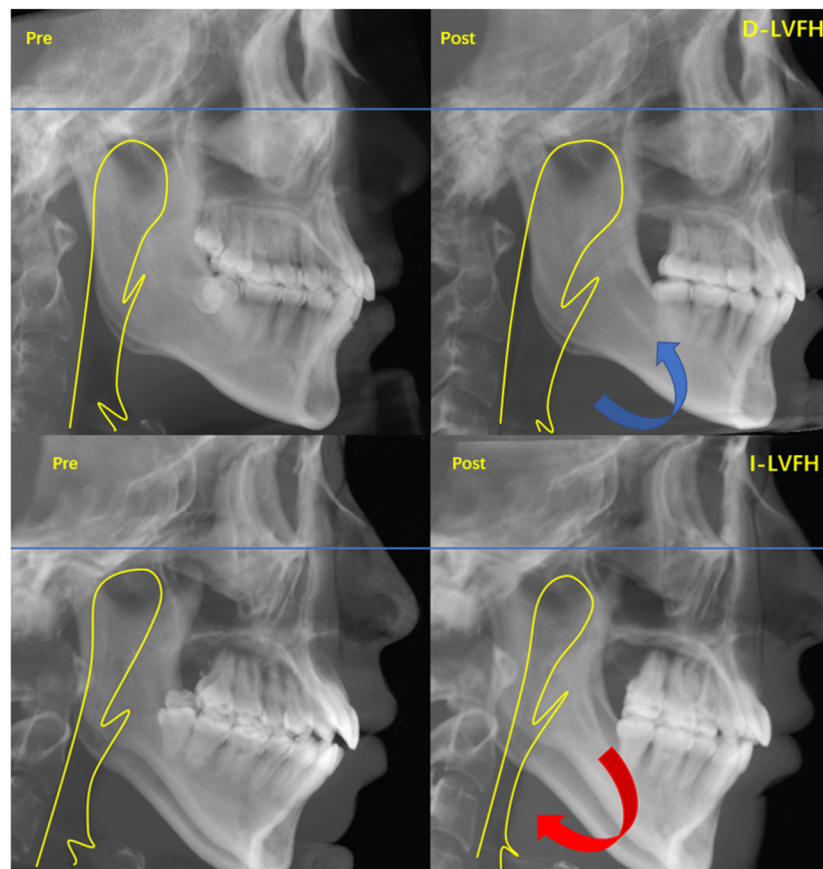


Fig 9. Anatomic changes of oropharyngeal airway in both groups: **A**, D-LVFH group; **B**, I-LVFH group.

Significant anterior displacement of the mandible was observed by evaluating the changes in SNB in the D-LVFH group; a similar change was not found in the I-LVFH group, suggesting that the counterclockwise rotation of the mandible produced by vertical control resulted in not only an upward movement but also a forward movement. The results also suggest that the improvement of the oropharyngeal airway may be due to a reduction of the LVFH and a forward jaw movement. Many previous studies have reported that vertical control improves vertical skeletal deformity, corrects open bite, and produces forward movement of the mentum.^{29,31-33} Consistent with the results of previous studies, our findings further demonstrated that vertical control was important for Class II hyperdivergent malocclusion treatment, as it improved skeletal deformity in both vertical and sagittal directions.

The anatomic characteristics reflect static changes in the upper airway to some extent. In this study, the D-LVFH group was the experimental group, and the I-LVFH group was the control group. Significant increases in volume and CSA_{\min} were observed in the D-LVFH

group, indicating that premolar extraction treatment with effective vertical control promoted oropharyngeal airway opening in patients with Class II hyperdivergent malocclusion. The variation in CSA_{\min} was 43 mm^2 in our study, which concurred with the results of a previous intragroup study. The previous study found a 47.17 mm^2 enlargement of the oropharyngeal airway after premolar extraction treatment and reported a significant positive correlation between the enlargements of CSA_{\min} and the upward movement of the mandible.¹⁴ The CSA_{\min} was significantly decreased in the I-LVFH group, suggesting that premolar extraction treatment with an increased lower vertical facial height may narrow the oropharyngeal airway. Cho et al³⁴ also found that the decreased glossopharynx after premolar extraction may be due to a clockwise rotation of the mandible. These findings suggest that an increased LVFH or clockwise rotation of the mandible should be avoided in the orthodontic treatment of patients with upper airway resistance syndrome. Although the above-mentioned previous studies found opposite results, both emphasized the influence of vertical control on the upper

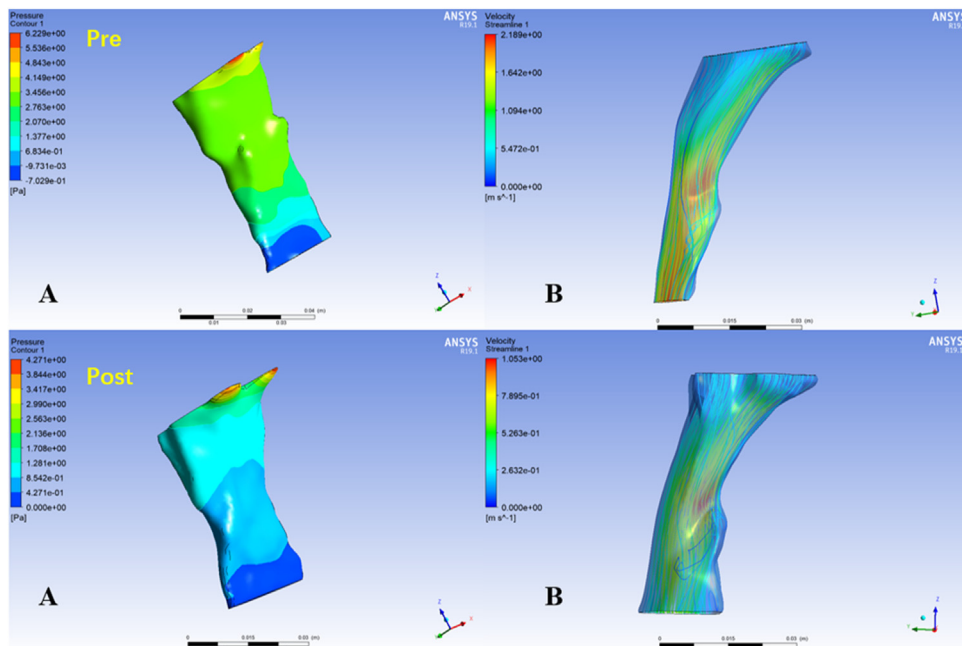


Fig 10. Comparison of aerodynamics during the inspiratory phase before and after treatment in the D-LVFH group: **A**, ΔP (ΔP , decrease); **B**, V_{max} (maximum velocity, decrease).

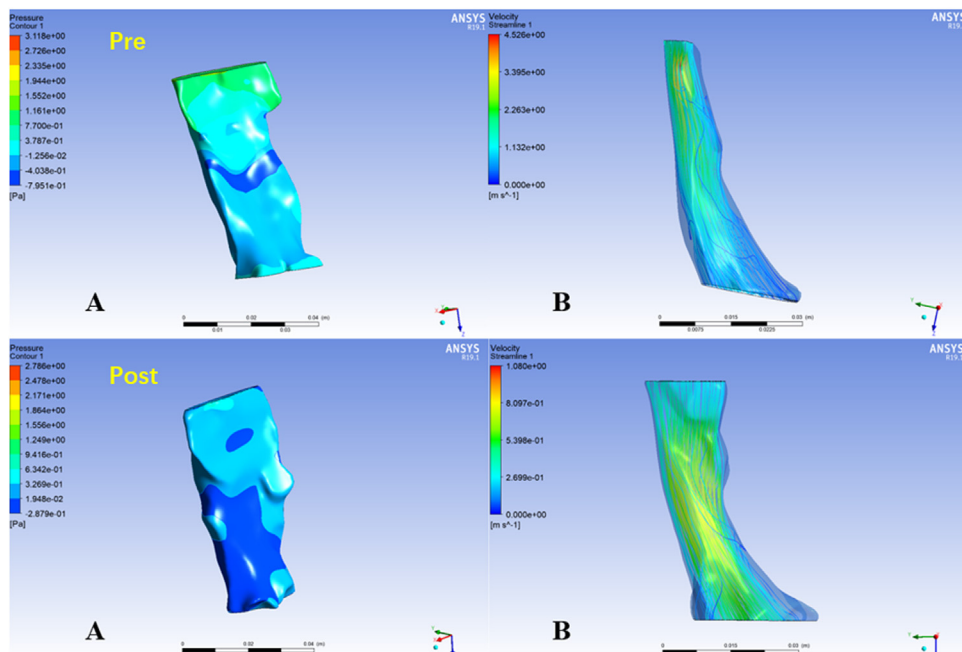


Fig 11. Comparison of aerodynamics during the expiratory phase before and after treatment in the D-LVFH group: **A**, ΔP (ΔP , decrease); **B**, V_{max} (maximum velocity, decrease).

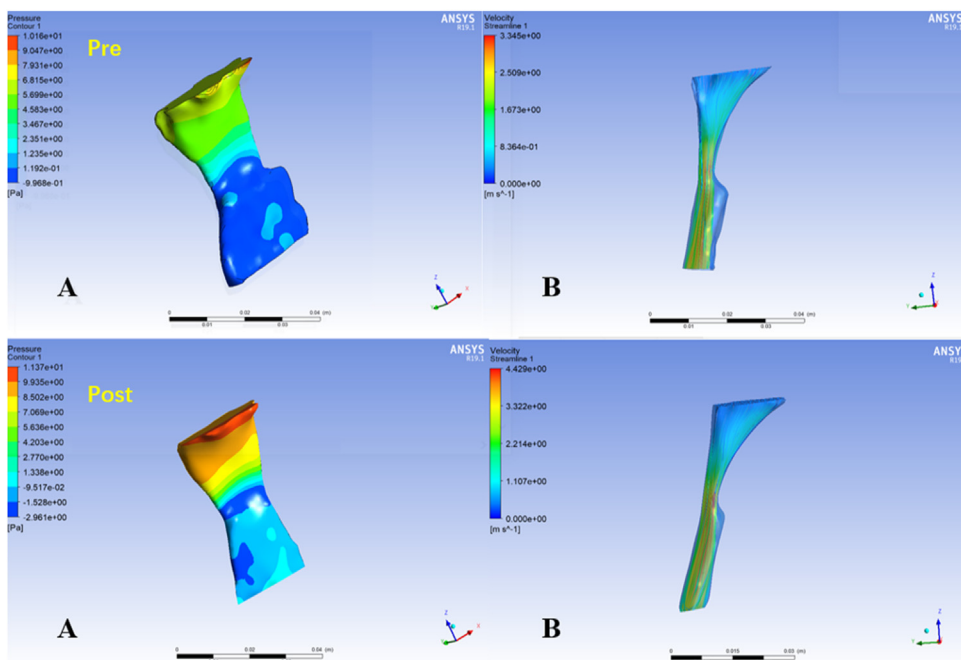


Fig 12. Comparison of aerodynamics during the inspiratory phase before and after treatment in the I-LVFH group: **A**, (ΔP , increase), ΔP ; **B**, V_{max} (maximum velocity, increase).

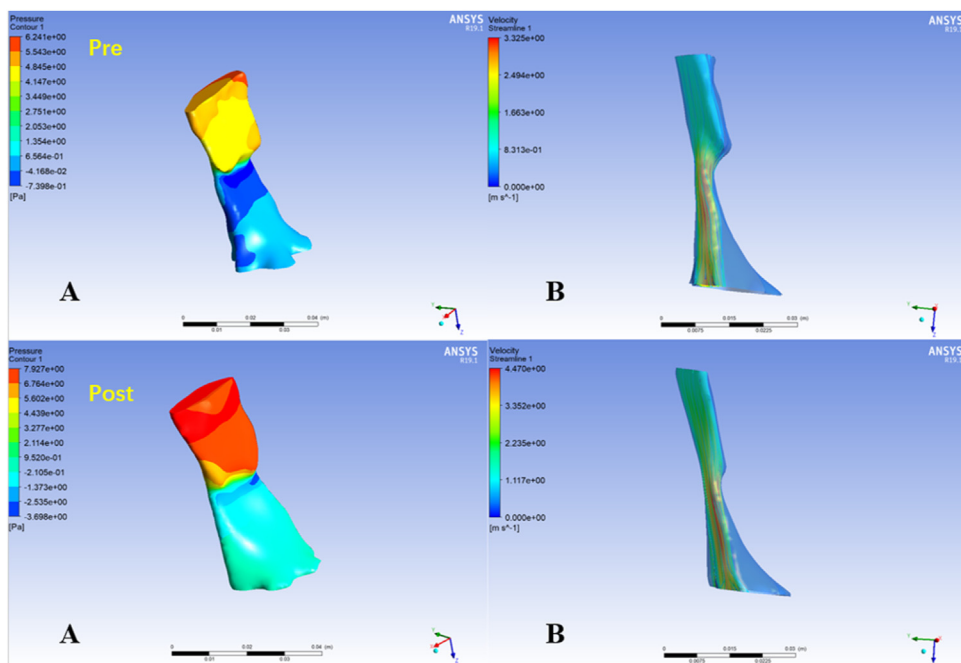


Fig 13. Comparison of aerodynamics during the expiratory phase before and after treatment in the I-LVFH group: **A**, ΔP ; **B**, V_{max} (maximum velocity, increase).

Table IV. Skeletal and dental variables of the D-LVFH and I-LVFH groups before and after treatment

Parameters	Pretreatment	Posttreatment	P value
D-LVFH group			
SNB (°)	75.43 ± 2.77	76.66 ± 2.24	<0.001*
U1/SN (°)	102.67 ± 6.32	98.61 ± 5.71	0.008*
U1-NA (mm)	5.02 ± 2.45	3.23 ± 1.67	0.002*
L1/MP (°)	96.36 ± 5.60	93.11 ± 6.64	0.001*
L1-NB (mm)	8.27 ± 2.85	6.78 ± 2.81	0.001*
U6-PP (mm)	23.86 ± 2.61	22.46 ± 2.40	<0.001*
L6-MP (mm)	32.26 ± 2.96	32.13 ± 2.82	0.565
ANS-Me (mm)	70.83 ± 5.32	68.77 ± 4.94	<0.001*
LVFH (mm)	65.60 ± 4.74	64.09 ± 4.65	<0.001*
MP/SN (°)	39.70 (9.80)	37.40 (8.10)	<0.001*
I-LVFH group			
SNB (°)	75.96 ± 2.27	75.93 ± 2.24	0.921
U1/SN (°)	106.56 ± 8.72	101.26 ± 8.01	0.006*
U1-NA (mm)	6.44 ± 2.20	4.81 ± 2.22	0.025*
L1/MP (°)	97.01 ± 7.75	93.43 ± 6.49	<0.001*
L1-NB (mm)	8.87 ± 2.28	7.31 ± 1.55	0.002*
U6-PP (mm)	23.61 ± 2.84	24.38 ± 2.40	0.016*
L6-MP (mm)	31.20 ± 3.25	31.56 ± 3.55	0.107
ANS-Me (mm)	68.18 ± 4.91	69.86 ± 4.82	0.003*
LVFH (mm)	64.06 ± 4.90	65.07 ± 4.88	<0.001*
MP/SN (°)	38.65 (6.70)	39.25 (6.82)	0.036*

Note. Values are presented as mean ± standard deviation for normal distributions and median (interquartile range) for nonnormal distributions. Paired *t* test was used for normal distributions and Wilcoxon signed rank test was used for nonnormal distributions.

*Statistically significant for *P* < 0.05.

airway during orthodontic treatment.^{14,34} In summary, premolar extraction treatment with effective vertical control benefits the anatomic characteristics of the upper airway after premolar extraction treatment.

Moreover, we did not observe a significant decrease in volume in the I-LVFH group, which was different from the decrease in CSA_{min}. The volume results in the I-LVFH group may indicate a trend rather than a statistically significant change. This trend is consistent with the study of Zhang et al¹³ on upper airway changes after orthodontic treatment. Zhang et al¹³ reported that the effect of premolar extraction treatment on the upper airway was not a reduction but a compensatory change and emphasized the compensatory role of the upper airway itself. The findings of Zhang et al¹³ conflicted with the results of other studies. For example, 2 previous studies reported that premolar extraction treatment for bimaxillary protrusion decreased the size of the upper airway.^{10,11} These studies suggested that premolar extractions reduced the oral volume and limited the tongue space, reducing the upper airway.^{10,11} We cannot accurately explain the reason for the differences between our findings and the previous studies. The potential reason may be the guidance of tongue position and habits. When we discover that patients have incorrect

tongue position or bad tongue habits, we correct their habits and guide their tongues to a specific position (against the front of the palate) during breathing and swallowing, which may prevent a significant reduction in upper airway volume, even if vertical facial height increases. However, we acknowledge that it is merely a hypothesis that needs to be verified by further systematic studies.

The aerodynamic characteristics somewhat reflect dynamic functional changes in the upper airway. Airway resistance (*R*) and maximum velocity (*V*_{max}) are fundamental parameters used to estimate the severity of OSA.^{19,25,35} In this study, we selected *R* and *V*_{max} as aerodynamic parameters to evaluate the dynamic function of the upper airway.

In the D-LVFH group, we found significant reductions in *R* in the inspiratory phase and *V*_{max} in the expiratory phase, whereas no significant changes were found in the I-LVFH group, suggesting that effective vertical control improved upper airway functions after premolar extraction treatment. The beneficial effects of premolar extraction treatment with effective vertical control on the function of the upper airway were demonstrated by simulating the airflow of the oropharyngeal airway using CFD, which has been widely used in upper airway assessment of patients with OSA, orthognathic surgery, and rapid maxillary expansion^{15,35,36} whereas few studies have reported changes in the aerodynamic characteristics of the upper airway after premolar extraction treatment. To the best of our knowledge, this study is the first to observe changes in the aerodynamic parameters of the oropharyngeal airway on the basis of CFD after premolar extraction treatment with vertical control.

We found significant differences in the aerodynamic and anatomic changes of the D-LVFH and I-LVFH groups. These findings may be explained by considering the opposite changes in the upper airway between the 2 groups. These opposite changes further illustrate the role of effective vertical control in improving the upper airway after premolar extraction treatment. A previous study showed that mandibular upward movement correlated with the increase of the upper airway in premolar extraction treatment through a comparison before and after treatment.¹⁴ Based on a previous study, we further demonstrated the beneficial effect of vertical control on the upper airway by comparing premolar extraction treatment in the D-LVFH and I-LVFH groups. Our findings suggest that the effects of vertical control should be ensured in hyperdivergent Class II malocclusion, not only for the improvement of skeletal and facial features but also for the improvement of the upper airway.

This study evaluated the upper airway using CBCT data captured in the upright position. Some studies

Table V. Anatomic and aerodynamic characteristics of the upper airway in the D-LVFH and I-LVFH groups before and after treatment

Parameters	Pretreatment	Posttreatment	P value
D-LVFH group-anatomic parameters			
Oropharyngeal volume (mm ³)	16,612.00 (4692.00)	20,857.00 (12,862.00)	0.002*
CSA _{min} (mm ²)	177.00 (147.00)	324.00 (219.00)	0.016*
Aerodynamic parameters			
Airway resistance during inspiration (Pa/L/min)	0.64 (0.79)	0.48 (0.44)	0.002*
Maximum velocity during inspiration (m × s ⁻¹)	2.19 (1.29)	1.81 (0.45)	0.063
Airway resistance during expiration (Pa/L/min)	0.60 (1.10)	0.46 (0.30)	0.061
Maximum velocity during expiration (m × s ⁻¹)	1.81 (2.03)	1.68 (0.68)	0.032*
I-LVFH group-anatomic parameters			
Oropharyngeal volume (mm ³)	18,985.00 (13,219.75)	14,256.00 (10,188.00)	0.098
CSA _{min} (mm ²)	179.00 (136.75)	148.50 (132.75)	0.039*
Aerodynamic parameters			
Airway resistance during inspiration (Pa/L/min)	0.46 (1.21)	0.56 (1.03)	0.408
Maximum velocity during inspiration (m × s ⁻¹)	1.60 (1.32)	1.63 (1.07)	0.326
Airway resistance during expiration (Pa/L/min)	0.53 (0.76)	0.68 (0.80)	0.460
Maximum velocity during expiration (m × s ⁻¹)	1.36 (1.62)	1.87 (1.54)	0.063

Note. All the data do not conform to normal distribution, so values are presented as median (interquartile range) and compared by Wilcoxon signed rank test.

*Statistically significant for $P < 0.05$.

Table VI. Comparison of changes between the D-LVFH and I-LVFH groups

Parameters	D-LVFH group	I-LVFH group	P value
Skeletal and dental parameters			
SNB (°)	1.23 ± 1.22	-0.03 ± 0.99	0.001*
U1/SN (°)	-4.05 ± 6.69	-5.29 ± 6.55	0.568
U1-NA (mm)	-1.78 ± 2.45	-1.63 ± 2.62	0.851
L1/MP (°)	-3.24 ± 3.94	-3.58 ± 3.12	0.768
L1-NB (mm)	-1.48 ± 1.75	-1.56 ± 1.65	0.881
U6-PP (mm)	-1.40 ± 1.02	0.77 ± 1.13	<0.001*
L6-MP (mm)	-0.13 ± 1.07	0.36 ± 0.84	0.118
ANS-Me (mm)	-2.06 ± 1.37	1.67 ± 1.93	<0.001*
LVFH (mm)	-1.51 ± 1.07	1.01 ± 0.83	<0.001*
MP/SN (°)	-2.10 (2.20)	0.30 (0.82)	<0.001*
Upper airway-anatomic parameters			
Oropharyngeal volume (mm ³)	2357.00 (6300.00)	-343.00 (7097.25)	<0.001*
CSA _{min} (mm ²)	43.00 (149.00)	-9.50 (54.75)	0.003*
Aerodynamic parameters			
Airway resistance during inspiration (Pa/L/min)	-0.15 (0.37)	0.06 (0.39)	0.008*
Maximum velocity during inspiration (m × s ⁻¹)	-0.27 (1.16)	0.05 (0.91)	0.043*
Airway resistance during expiration (Pa/L/min)	-0.10 (0.46)	0.01 (0.46)	0.121
Maximum velocity during expiration (m × s ⁻¹)	-0.24 (1.27)	0.30 (0.46)	0.005*

Note. Values are presented as mean ± standard deviation for normal distributions and median (interquartile range) for nonnormal distributions. Independent sample *t* test was used for normal distributions, and the Wilcoxon rank sum test was used for nonnormal distributions.

*Statistically significant for $P < 0.05$.

have reported differences in upper airway morphology and functionality between the upright and supine positions.³⁷ Importantly, the airway may be significantly smaller when patients were in a supine position compared with an upright position.³⁸ Further investigations should evaluate the changes in the upper airway after premolar extraction treatment with vertical control based on CBCT data in the supine position.

BMI may affect the physiological respiratory function of patients. We did not collect data on BMI after treatment. Instead, we observed the frontal photographs of the patients to confirm that there was a negligible difference in the figures of the patients before and after treatment. In addition, the morphology and function of the upper airway are closely related to the quality of sleep.^{5,6} From the sleep perspective, we did not perform sleep

breathing assessments, such as polysomnography. Further analyses of relevant sleep breathing assessments are warranted.

CONCLUSIONS

1. Effective vertical control decreases the LVFH and facilitates a counterclockwise rotation of the mandible, which might improve the anatomic and aerodynamic characteristics of the oropharyngeal airway after premolar extraction treatment.
2. Vertical control is an important treatment to improve skeletal features and oropharyngeal airway in patients with Class II hyperdivergent malocclusion with nonsevere crowding.

AUTHOR CREDIT STATEMENT

Hongyi Tang contributed to investigation, conceptualization, formal analysis, data curation, methodology, software, and original draft preparation; Xinyu Cui contributed to resources; Huazhi Li contributed to resources; Fu Zheng contributed to investigation; Youchao Chen contributed to investigation; and Jiuhui Jiang contributed to resources, project administration, supervision, and manuscript review and editing.

SUPPLEMENTARY DATA

Supplementary data associated with this article can be found, in the online version, at <https://doi.org/10.1016/j.ajodo.2023.05.003>.

REFERENCES

1. Sleep-related breathing disorders in adults: recommendations for syndrome definition and measurement techniques in clinical research. The report of an American Academy of Sleep Medicine task force. *Sleep* 1999;22:667-89.
2. Destors M, Tamisier R, Galerneau LM, Lévy P, Pepin JL. Pathophysiology of obstructive sleep apnea syndrome and its cardiometabolic consequences. *Presse Med* 2017;46:395-403.
3. Li M, Li X, Lu Y. Obstructive sleep apnea syndrome and metabolic diseases. *Endocrinology* 2018;159:2670-5.
4. Pham LV, Schwartz AR. The pathogenesis of obstructive sleep apnea. *J Thorac Dis* 2015;7:1358-72.
5. Lee RWW, Sutherland K, Cistulli PA. Craniofacial morphology in obstructive sleep apnea: a review. *Clin Pulm Med* 2010;17:189-95.
6. Katyal V, Pamula Y, Martin AJ, Daynes CN, Kennedy JD, Sampson WJ. Craniofacial and upper airway morphology in pediatric sleep-disordered breathing: systematic review and meta-analysis. *Am J Orthod Dentofacial Orthop* 2013;143:20-30.e3.
7. Deng J, Gao X. A case-control study of craniofacial features of children with obstructed sleep apnea. *Sleep Breath* 2012;16:1219-27.
8. Sutherland K, Lee RW, Cistulli PA. Obesity and craniofacial structure as risk factors for obstructive sleep apnoea: impact of ethnicity. *Respirology* 2012;17:213-22.
9. Lee RW, Vasudavan S, Hui DS, Prvan T, Petocz P, Darendeliler MA, et al. Differences in craniofacial structures and obesity in Caucasian and Chinese patients with obstructive sleep apnea. *Sleep* 2010;33:1075-80.
10. Bhatia S, Jayan B, Chopra SS. Effect of retraction of anterior teeth on pharyngeal airway and hyoid bone position in Class I bimaxillary dentoalveolar protrusion. *Med J Armed Forces India* 2016;72(Suppl 1):S17-23.
11. Chen Y, Hong L, Wang CL, Zhang SJ, Cao C, Wei F, et al. Effect of large incisor retraction on upper airway morphology in adult bimaxillary protrusion patients. *Angle Orthod* 2012;82:964-70.
12. Wang Q, Jia P, Anderson NK, Wang L, Lin J. Changes of pharyngeal airway size and hyoid bone position following orthodontic treatment of Class I bimaxillary protrusion. *Angle Orthod* 2012;82:115-21.
13. Zhang J, Chen G, Li W, Xu T, Gao X. Upper airway changes after orthodontic extraction treatment in adults: A preliminary study using cone beam computed tomography. *PLoS One* 2015;10:e0143233.
14. Shi X, Chen H, Lobbezoo F, Berkhout E, de Lange J, Guo J, et al. Effects of miniscrew-assisted orthodontic treatment with premolar extractions on upper airway dimensions in adult patients with Class II high-angle malocclusion. *Am J Orthod Dentofacial Orthop* 2021;159:724-32.
15. Deng JR, Li YA, Wang XD, Li J, Ding Y, Zhou YH. Evaluation of long-term stability of vertical control in hyperdivergent patients treated with temporary anchorage devices. *Curr Med Sci* 2018;38:914-9.
16. Tang H, Liu P, Xu Q, Hou Y, Guo J. A comparative analysis of aerodynamic and anatomic characteristics of upper airway before and after mini-implant-assisted rapid maxillary expansion. *Am J Orthod Dentofacial Orthop* 2021;159:e301-10.
17. Christino M, Vinha PP, Faria AC, Garcia DM, de Mello-Filho FV. Impact of counterclockwise rotation of the occlusal plane on the mandibular advancement, pharynx morphology, and polysomnography results in maxillomandibular advancement surgery for the treatment of obstructive sleep apnea patients. *Sleep Breath* 2021;25:2307-13.
18. Luo H, Sin S, McDonough JM, Isasi CR, Arens R, Wootton DM. Computational fluid dynamics endpoints for assessment of adenotonsillectomy outcome in obese children with obstructive sleep apnea syndrome. *J Biomech* 2014;47:2498-503.
19. Powell NB, Mihaescu M, Mylavarapu G, Weaver EM, Guillemainault C, Gutmark E. Patterns in pharyngeal airflow associated with sleep-disordered breathing. *Sleep Med* 2011;12:966-74.
20. Mihaescu M, Mylavarapu G, Gutmark EJ, Powell NB. Large eddy simulation of the pharyngeal airflow associated with obstructive sleep apnea syndrome at pre and post-surgical treatment. *J Biomech* 2011;44:2221-8.
21. Zheng Z, Liu H, Xu Q, Wu W, Du L, Chen H, et al. Computational fluid dynamics simulation of the upper airway response to large incisor retraction in adult Class I bimaxillary protrusion patients. *Sci Rep* 2017;7:45706.
22. Bazina M, Cevidanes L, Ruellas A, Valiathan M, Quereshey F, Syed A, et al. Precision and reliability of Dolphin 3-dimensional voxel-based superimposition. *Am J Orthod Dentofacial Orthop* 2018;153:599-606.
23. Pauwels R, Jacobs R, Singer SR, Mupparapu M. CBCT-based bone quality assessment: are Hounsfield units applicable? *Dentomaxillofac Radiol* 2015;44:20140238.
24. DenOtter TD, Schubert J. Hounsfield Unit. Treasure Island. StatPearls Publishing; 2019.

25. Rana SS, Kharbanda OP, Agarwal B. Influence of tongue volume, oral cavity volume and their ratio on upper airway: a cone beam computed tomography study. *J Oral Biol Craniofac Res* 2020;10:110-7.
26. Chen H, Aarab G, Parsa A, de Lange J, van der Stelt PF, Lobbezoo F. Reliability of three-dimensional measurements of the upper airway on cone beam computed tomography images. *Oral Surg Oral Med Oral Pathol Oral Radiol* 2016;122:104-10.
27. Younis BA, Berger SA. A turbulence model for pulsatile arterial flows. *J Biomech Eng* 2004;126:578-84.
28. Zhao M, Barber T, Cistulli P, Sutherland K, Rosengarten G. Computational fluid dynamics for the assessment of upper airway response to oral appliance treatment in obstructive sleep apnea. *J Biomech* 2013;46:142-50.
29. Van Holsbeke C, De Backer J, Vos W, Verdonck P, Van Ransbeeck P, Claessens T, et al. Anatomical and functional changes in the upper airways of sleep apnea patients due to mandibular repositioning: a large scale study. *J Biomech* 2011;44:442-9.
30. Chiang CC, Jeffres MN, Miller A, Hatcher DC. Three-dimensional airway evaluation in 387 subjects from one university orthodontic clinic using cone beam computed tomography. *Angle Orthod* 2012;82:985-92.
31. Deguchi T, Kurosaka H, Oikawa H, Kuroda S, Takahashi I, Yamashiro T, et al. Comparison of orthodontic treatment outcomes in adults with skeletal open bite between conventional edgewise treatment and implant-anchored orthodontics. *Am J Orthod Dentofacial Orthop* 2011;139(4):S60-8.
32. Arai C, Choi JW, Nakaoka K, Hamada Y, Nakamura Y. Management of open bite that developed during treatment for internal derangement and osteoarthritis of the temporomandibular joint. *Korean J Orthod* 2015;45:136-45.
33. Jung MH. Vertical control of a Class II deep bite malocclusion with the use of orthodontic mini-implants. *Am J Orthod Dentofacial Orthop* 2019;155:264-75.
34. Cho HN, Yoon HJ, Park JH, Park YG, Kim SJ. Effect of extraction treatment on upper airway dimensions in patients with bimaxillary skeletal protrusion relative to their vertical skeletal pattern. *Korean J Orthod* 2021;51:166-78.
35. Mihaescu M, Murugappan S, Gutmark E, Donnelly LF, Khosla S, Kalra M. Computational fluid dynamics analysis of upper airway reconstructed from magnetic resonance imaging data. *Ann Otol Rhinol Laryngol* 2008;117:303-9.
36. Chen H, Li Y, Reiber JH, de Lange J, Tu S, van der Stelt P, et al. Analyses of aerodynamic characteristics of the oropharynx applying CBCT: obstructive sleep apnea patients versus control subjects. *Dentomaxillofac Radiol* 2018;47:20170238.
37. Van Holsbeke CS, Verhulst SL, Vos WG, De Backer JW, Vinchurkar SC, Verdonck PR, et al. Change in upper airway geometry between upright and supine position during tidal nasal breathing. *J Aerosol Med Pulm Drug Deliv* 2014;27:51-7.
38. Camacho M, Capasso R, Schendel S. Airway changes in obstructive sleep apnoea patients associated with a supine versus an upright position examined using cone beam computed tomography. *J Laryngol Otol* 2014;128:824-30.